



OPEN

SUBJECT AREAS:

FLUORESCENCE
IMAGING

MIRNAS

Received
17 February 2014Accepted
21 March 2014Published
9 April 2014Correspondence and
requests for materials
should be addressed to
S.K. (kimsoohag@
empal.com)

A color-tunable molecular beacon to sense miRNA-9 expression during neurogenesis

Hae Young Ko, Jonghwan Lee, Jin Young Joo, Yong Seung Lee, Hyejung Heo, Jung Jae Ko & Soonhag Kim

Department of Biomedical Science, College of Life Science, CHA University, 605-21 Yeoksam 1-dong, Gangnam-gu, Seoul 135-081, Republic of Korea.

A typical molecular beacon (MB) composing of a fluorophore and a quencher has been used to sense various intracellular biomolecules including microRNAs (miRNA, miR). However, the on/off-tunable miRNA MB is difficult to distinguish whether the observed low fluorescence brightness results from low miRNA expression or low transfection of the miRNA MB. We developed a color-tunable miRNA-9 MB (Color9 MB) to sense miR-9 expression-dependent color change. The Color9 MB was synthesized by a partially double-stranded DNA oligonucleotide containing a miR-9 binding site and a reporter probe with Cy3/black hole quencher 1 (BHQ1) at one end and a reference probe with Cy5.5 at the other end. The Color9 MB visualized CHO and P19 cells with red color in the absence of miR-9 and yellow color in the presence of miR-9. *In vivo* imaging demonstrated that the green fluorescence recovery of the reporter probe from the Color9 MB increased gradually during neuronal differentiation of P19 cells, whereas red fluorescence activity of the reference probe remained constant. These results showed the great specificity of sensing miR-9 expression- and neurogenesis-dependent color change.

Molecular beacon (MB) probes have been widely used in chemistry, biology, biotechnology and medical sciences for biomolecule recognition due to their ease of synthesis, unique functionality, molecular specificity and structural tolerance to various modifications¹⁻³. A typical MB is composed of a short stem loop-structured DNA oligonucleotide that has a quenching molecule and fluorescent dye at the end of each oligonucleotide⁴. The loop sequences are complementary to target molecules including DNA or RNA. In the absence of a target molecule, fluorescence is absorbed by quenching molecules as a result of fluorescence resonance energy transfer (FRET) between the fluorescent dye and the quencher. However, if the target molecule binds to the loop structure of the MB, the quencher molecules separate from the fluorescent dye resulting in a bright fluorescence signal.

MiRNA (miRNA, miR) is a class of small noncoding RNAs that play a key role as a suppressor of its target gene during cellular processes and diseases^{5,6}. The MB principle has recently been applied to image miRNAs because of the need to diagnose miRNA-involving cellular developments and diseases including cancers^{7,8}. These MB-based miRNA imaging systems successfully and non-invasively visualize miRNA biogenesis in cells and living organisms. The miRNA MB sensor could overcome the limitation of a bioluminescent reporter gene-based miRNA imaging system by providing a signal-on imaging signal in the presence of the miRNA. The bioluminescent miRNA reporter gene frequently suffers from an inability to distinguish the miRNA function-regulating signal-off imaging signals from cellular loss⁹⁻¹². Compared with most current methods to analyze miRNA expression including real-time polymerase chain reaction (RT-PCR), northern blot and microarray¹³⁻¹⁵, which require cell lysis, the miRNA MB imaging system provides accurate information about miRNA expression in a single living cell and non-invasively repeats on the same subjects, which is critical to understand the functions of miRNAs in biology and medicine. However, the miRNA MB sensor, which is composed of a single fluorophore on one end and a single quencher on the other end, simply represents mono fluorescence-dependent signal-on or-off imaging in response to miRNA expression. This on/off-tunable miRNA MB is limited to accurately sense a real-time dynamic change in a target miRNA when fluorescence brightness is weak in cells. Therefore, a color-tunable miRNA MB with two different fluorophores in which one is sensitive to miRNA and the other is insensitive with miRNA can overcome the limitation of previously developed miRNA MB sensors by providing miRNA expression-dependent color changes.



In this study, we developed a color-tunable miRNA MB sensor to image intracellular miR-9 expression (designated as ColoR9 MB). The *in vitro* and *in vivo* color-tunable molecular imaging of miR-9-regulating neurogenesis was conducted using P19 cells (a mouse embryonic teratocarcinoma cell lines).

Results

Design and mechanism of the ColoR9 MB. The ColoR9 MB was synthesized with a linear structured and partially double-stranded DNA oligonucleotide (Fig. 1). The long oligonucleotide had a miR-9 binding sequence that was complementary to the mature miR-9 and labeled with two different fluorophores. The two fluorophores were Cy3 (excitation/emission: 546/563 nm, green) at the 5' end as a reporter probe (called miR-9 sensitive dye) and Cy5.5 (excitation/emission: 683/705 nm, red) at the 3' end as a reference probe (called miR-9 insensitive dye). In addition, the long oligonucleotide had a long overhang sequence between the miR-9 binding sequence and Cy5.5 to allow sufficient distance so that the reference probe was not influenced by the quencher. A short DNA oligonucleotide which was complementary to the 5' end of the long DNA oligonucleotide had a black hole quencher 1 (BHQ1) at the 3' end (designated as the quencher oligonucleotide) and was partially hybridized with the long oligonucleotide to form the ColoR9 MB. The hypothesis for sensing a miR-9 expression-dependent color change using the ColoR9 MB is provided below. First, in the absence of miR-9, fluorescence activity of the miR-9 sensitive dye from the ColoR9 MB is visualized by green and is efficiently quenched due to the close proximity between Cy3 and BHQ1. This results in absorption of the emitted fluorescence into the quencher by FRET¹⁶, which eventually visualizes only red from miR-9 insensitive dye of the ColoR9 MB that is constantly emitted regardless of the miR-9 expression. In the presence of miR-9, the reporter probe is activated by binding of miR-9 to the miR-9 binding site and detaching the quencher oligonucleotide from the ColoR9 MB. Thus, green fluorescence activity is recovered, resulting in a yellow color due to the merge of green from the Cy3 and red from Cy5.5.

Color-tunable specificity of sensing the miR-9 using the ColoR9 MB. Optimal quenching efficiency of the ColoR9 MB was first

determined on a black plate to determine the specificity of sensing the miR-9 expression-dependent color change. The IVIS[®] spectrum imaging system demonstrated that incubating a fixed concentration of the long oligonucleotide (10 pmol) with a gradual increase in the concentration (0, 1, 5, 10, and 20 pmol) of the quencher oligonucleotide resulted in significantly decreased quenching from the reporter probe, whereas fluorescence signals of the reference probe from various concentrations of the quencher were constant, indicating successful formation of the ColoR9 MB (Supplementary Fig. 1A). The maximum quenching efficiency of the reporter probe reached about 40% at 10 pmol of the quencher oligonucleotide (Fig. 2A).

When the ColoR9 MB was incubated with various concentrations (0, 1, 10, and 30 pmol) of exogenous miR-9 on a black plate, a gradual increase in fluorescence recovery of the miR-9 sensitive Cy3 dye occurred, whereas incubation of 30 pmol of miR-1 (used as a control) continued to quench the fluorescence signals of the reporter probe (Fig. 2B and Supplementary Fig. 1B). As expected, the Cy5.5 reference probe from the ColoR9 MB showed no significant change in fluorescence intensity both with and without incubation with miR-9 or miR-1. Incubating the ColoR9 MB in PBS, opti-MEM media, and with CHO cells demonstrated good stability up to 2 days by showing quenching efficiency of the reporter probe in the absence of miR-9 and fluorescence recovery in the presence of miR-9 (Supplementary Fig. 2 and 3). The miR-9 insensitive dye of the ColoR9 MB showed constant fluorescence intensity in PBS, opti-MEM media, and CHO cells for up to 2 days regardless of miR-9 incubation.

To further demonstrate the specificity of miR-9 sensing in cells, the ColoR9 MB (30 pmol) was co-transfected with exogenous miR-9 into CHO cells, which do not express miR-9 (Supplementary Fig. 4). The quantitative fluorescence signals of the reporter probe from the ColoR9 MB, in the absence of exogenous miR-9 and in the presence of exogenous miR-1 remained in the quenched state (Fig. 2C). The fluorescence activity of the miR-9 sensitive dye significantly and gradually increased with various concentrations (0, 10, and 30 pmol) of the exogenous miR-9 in CHO cells. The reference probe of the ColoR9 MB provided a constant fluorescence signal regardless of incubation with miR-9 or miR-1. Confocal microscopic imaging of CHO cells transfected with the ColoR9 MB showed that the bright

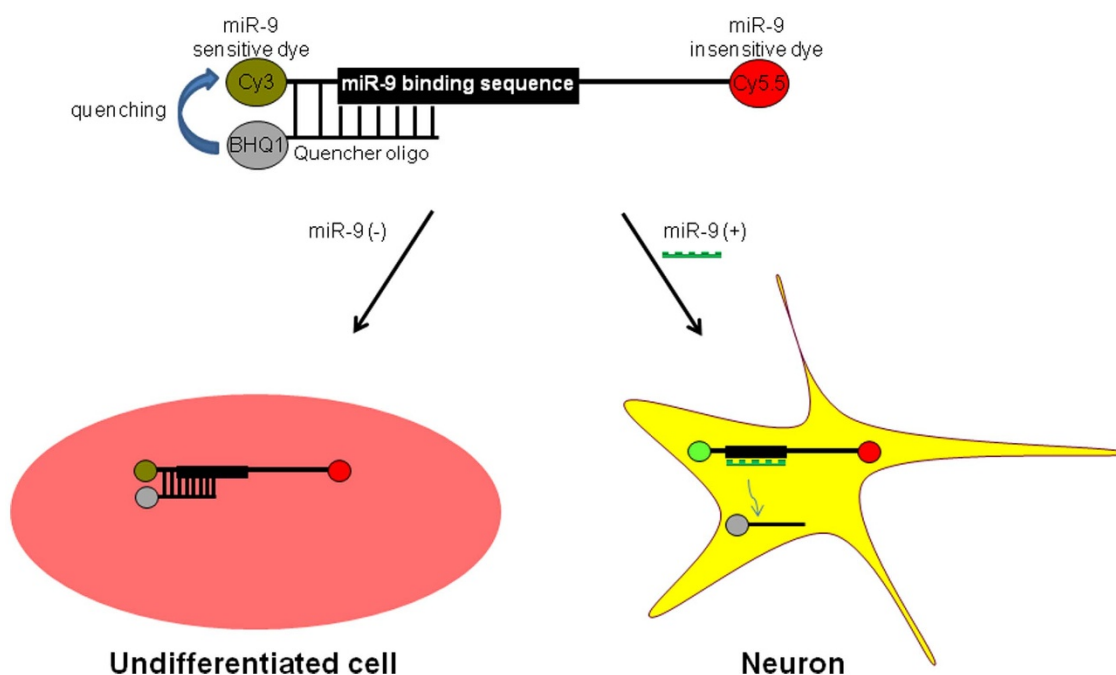


Figure 1 | Schematic illustration of the ColoR9 MB for sensing miR-9 expression-dependent color change.

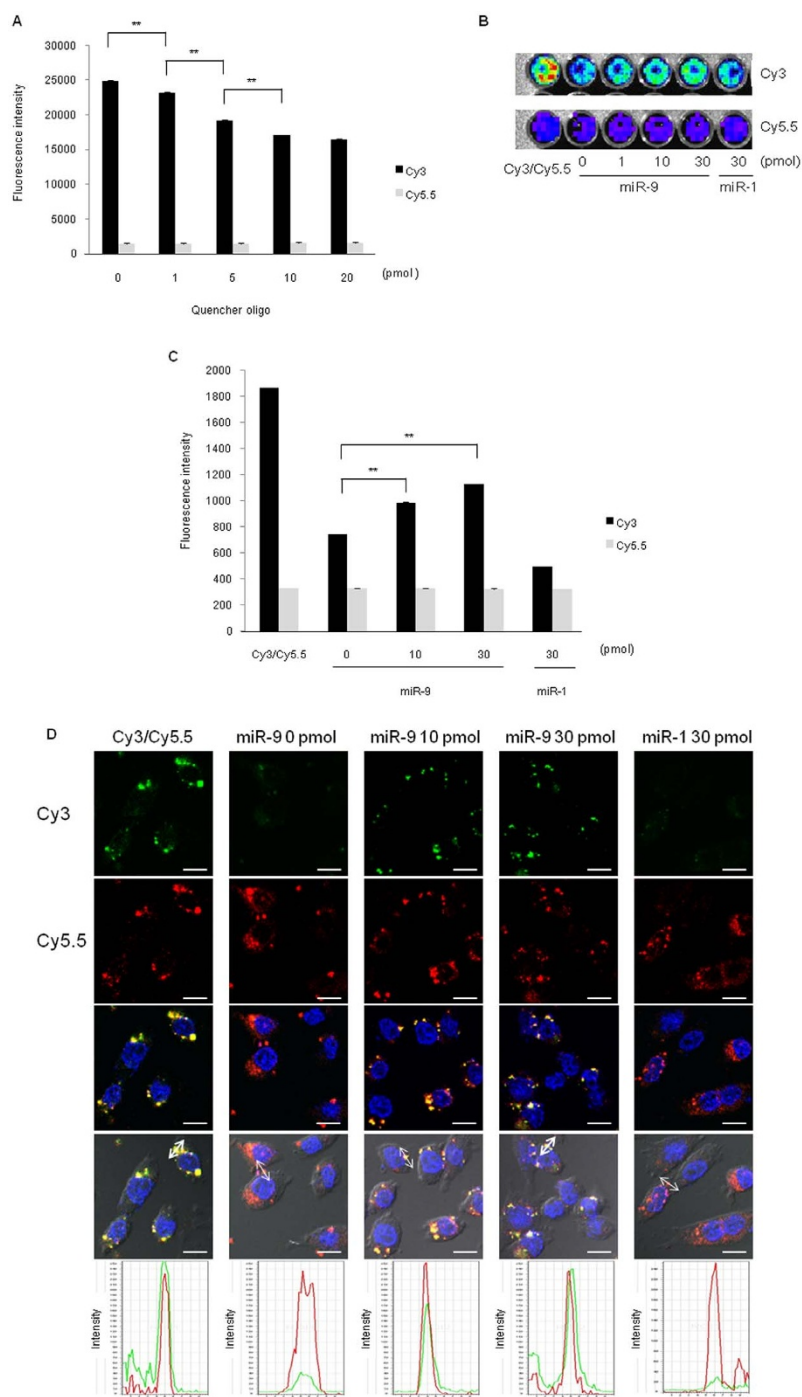


Figure 2 | Specificity of the ColoR9 MB to sense miR-9 expression. (A) Quenching efficiency of the reporter probe in the ColoR9 MB. Fluorescence intensity of Cy3 (the reporter probe) and Cy5.5 (the reference probe) in the long oligonucleotide (10 pmol) was measured by incubating various concentrations (0, 1, 5, 10, and 20 pmol) of the quencher oligonucleotide on a black plate. Data are expressed as means \pm standard deviations of triplicate samples (** $P < 0.005$). (B) The Cy3 and Cy5.5 fluorescence images of the ColoR9 MB in the presence of miR-9. Various concentrations (0, 1, 10, and 30 pmol) of miR-9 and 30 pmol of miR-1 (used as a negative control) were incubated with 30 pmol of the ColoR9 MB on the plate. 30 pmol of the long oligonucleotide (indicated as Cy3/Cy5.5) was used a positive control. (C) Fluorescence intensity of the ColoR9 MB in CHO cells. Three different concentrations (0, 10, and 30 pmol) of miR-9 and 30 pmol of miR-1 were co-transfected with 30 pmol of the ColoR9 MB into CHO cells. 30 pmol of the long oligonucleotide (indicated as Cy3/Cy5.5) transfected into CHO cells was used a control. Cy3 and Cy5.5 fluorescence intensities are displayed as means \pm standard deviations of triplicate samples (** $P < 0.005$). (D) Confocal microscopic analysis of the ColoR9 MB in CHO cells. CHO cells treated with the ColoR9 MB were transfected with 30 pmol of the long oligonucleotide (first column), three different concentrations (0, 10, and 30 pmol of miR-9 or 30 pmol of miR-1). The fluorescence images of the reporter probe (Cy3, green, first row) were acquired at excitation of 546 nm and emission of 563 nm. Confocal microscopic images of the reference probe (Cy5.5, red, second row) were obtained at excitation of 683 nm and emission of 705 nm. The third and fourth rows are merged with the 4',6-diamidino-2-phenylindole (DAPI) image (nucleus staining, 460 nm) and cellular morphology, respectively. Yellow color was obtained by merging green and red. The fifth row is the line scan showing fluorescence intensity of Cy3 (green) and Cy5.5 (red) along the line shown in the fourth row. Scale bar, 10 μ m.



green from the reporter probe was clearly quenched in the cytoplasm without additional incubation of exogenous miR-9 and with treatment of exogenous miR-1 (Fig. 2D). When exogenous miR-9 was co-transfected into CHO cells, the green fluorescence signals of the miR-9 sensitive Cy3 dye increased in a dose-dependent manner from the cell cytoplasm. The green fluorescence recovery was acquired by hybridization of miR-9 to the miR-9 binding site and detachment of the quencher oligonucleotide from the ColoR9 MB. However, red fluorescence of the miR-9 insensitive Cy5.5 dye was visualized constantly in the CHO cell cytoplasm regardless of miR-9 or miR-1 transfection. Therefore, CHO cells with the transfection of the ColoR9 MB were visualized as red in the absence of the miR-9, and yellow was obtained by the merging of green and red in the presence of miR-9. Similarly, a line scan analysis of the region of interest (ROI) by confocal microscopy of CHO cells further confirmed that the fluorescence color change of the ColoR9 MB from red to yellow resulted from the gradual increase in miR-9 expression-dependent green fluorescence recovery of the reporter probe. These results demonstrate the high sensing specificity of the miR-9 expression-dependent color change using the ColoR9 MB.

Color-tunable imaging of endogenous miR-9 expression during P19 cells neurogenesis. To image the endogenous miR-9 expression-dependent color change during neurogenesis, we first induced P19 cells neuronal differentiation with retinoic-acid (RA) in culture media and confirmed differentiation by immunocytochemistry with increased Tuj1 (a neuronal marker) expression and decreased Oct4 (stem cell marker) expression (Supplementary Fig. 5). The qRT-PCR demonstrated that the endogenous mature miR-9 increased gradually during neuronal differentiation of P19 cells (Supplementary Fig. 4). To determine if the ColoR9 MB transfected into P19 cells inhibited the expression and function of the endogenous miR-9, we investigated the endogenous level of miR-9 and the REST-silencing transcription factor (REST) gene that functions as a neuronal repressor and is an endogenous target of miR-9¹⁷. The miR-9 expression generally increased during neurogenesis and REST was down-regulated by miR-9 function. Real-time PCR showed that the normal endogenous expression pattern of both miR-9 and REST was not significantly affected by up to 30 pmol of the ColoR9 MB transfected into 4-day-post-differentiated P19 cells, compared with that from 4-day-post-differentiated P19 cells that were not treated with the ColoR9 MB (Supplementary Fig. 6A and B). The ColoR9 MB (50 and 100 pmol) transfected into 4-day-post-differentiated P19 cells showed a significant decrease in miR-9 expression and a slight increase in REST expression. These results suggest that transfection with 30 pmol of the ColoR9 MB into P19 cells sensed intact expression of the endogenous miR-9 during neurogenesis without affecting miR-9 expression and function. When the ColoR9 MB (30 pmol) was transfected into P19 cells, the quantitative fluorescence intensity of the reporter probe on days 2 and 4 after neuronal differentiation of P19 cells was slightly and highly increased, respectively, compared with that from undifferentiated P19 cells (Fig. 3A). Additional treatment with a miR-9 antagonist, which is a synthetic oligonucleotide that fully complements the miR-9 nucleotide sequences, inhibited hybridization of the endogenous miR-9 to the miR-9 binding site and repressed the fluorescence recovery of the reporter probe 4 days after neurogenesis of P19 cells transfected with the ColoR9 MB. The quantitative fluorescence activity of the reference probe was constant regardless of neuronal differentiation of P19 cell with or without additional treatment with the miR-9 antagonist. Confocal microscopic imaging of P19 cells transfected with the ColoR9 MB demonstrated that bright green fluorescence remained quenched in the cytoplasm of the undifferentiated P19 cells and 4-day-post-differentiated P19 cells following transfection with the miR-9 antagonist (Fig. 3B). However, the miR-9 sensitive Cy3 dye increased gradually in green fluorescence

from the cytoplasm of P19 cells on days 2 and 4 after RA treatment, due to the gradual increase in the expression level of the endogenous miR-9 during P19 cell neurogenesis. From the color mixture of the miR-9 sensitive Cy3 dye with the miR-9 insensitive Cy5.5 dye, which showed invariable red brightness during neurogenesis of P19 cells, the miR-9 expression-dependent color-tunable imaging by the ColoR9 MB visualized undifferentiated P19 cells as red, 2-day-post-differentiated P19 cells as reddish yellow, and 4-day-post-differentiated P19 cells as yellow. The line scan analysis of the ROI by confocal microscopy further confirmed the gradual increase in green fluorescence recovery of the reporter probe and constant fluorescence intensity of the reference probe during P19 cell neurogenesis. The fluorescence patterns of the reporter probe and the reference probe during neurogenesis of P19 cells further confirmed the uneven distribution and gradual increase in miR-9 expression by entire cell ROI measurement of the ColoR9 MB (Supplementary Fig. 7).

To obtain an *in vivo* image of miR-9 during neurogenesis, 1×10^7 P19 cells transfected with the ColoR9 MB were implanted subcutaneously in both thighs of nude mice. Only P19 cells grafted into the right thigh were treated with RA and were induced into neuronal differentiation. The Cy5.5 fluorescence intensity of the reference probe was strongly and constantly observed from both the left and right thighs of nude mice for 2 days regardless of P19 cell neuronal differentiation (Fig. 3C). However, the Cy3 fluorescence of the miR-9 sensitive dye increased gradually in the right thigh over 2 days due to the gradual increase in miR-9 expression during P19 cell neurogenesis, while the left thigh remained in the invariably quenched fluorescence state of the reporter probe. The fold ratio determined by the left and the right thighs from the ROI analysis showed that the emission intensity of the reporter probe 1 and 2 days after neurogenesis was about 1.3-fold and 1.8-fold higher than that from day 0 (Supplementary Fig. 8). The fold ratio of the ROI analysis demonstrated no significant change in the reference probe during the 2 days of P19 cell neuronal differentiation. *Ex vivo* imaging of tissues isolated from both thighs 2 days after implantation of P19 cells confirmed the increase in fluorescence intensity of the reporter probe and invariable fluorescence brightness of the reference probe before and after neurogenesis (Supplementary Fig. 9 and 10). An immunohistochemical analysis of the isolated P19 cells from both thighs using Tuj1 and Oct4 antibodies confirmed neurogenesis progression *in vivo* (Supplementary Fig. 11). The gradual fluorescence recovery of the reporter probe from the right thigh was due to miR-9-regulating neurogenesis of P19 cells.

Discussion

Bioimaging of intracellular molecular mechanisms including transcription, translation, location, and function of genes is very important for early and accurate diagnosis of cellular developments and diseases. However, most molecular imaging studies have used optical, radioisotope, and magnetic resonance imaging probes and have focused on targeting genes expressed on the cellular membrane rather than inside cells. A molecular imaging probe for intracellular genes must be easy to use to discriminate targets from other biomolecules. MB has been successfully used to visualize the expression and function of intracellular biomolecules including miRNAs by providing a highly specific on/off-tunable sensing system^{7,8}. However, it is frequently difficult to distinguish a dynamic change in target molecules with an on/off-tunable MB sensor when fluorescence is weak in cells due to low transfection of the MBs or weak target molecule expression. A color-tunable MB that can provide a target molecule expression-dependent color change is necessary to overcome this limitation of the on/off-tunable MB sensor. However, a conventional color-tunable MB that successfully detected an mRNA¹⁸ can produce nonspecific background signal or false positive results due to its stem-loop structure which causes the quenching molecule to be

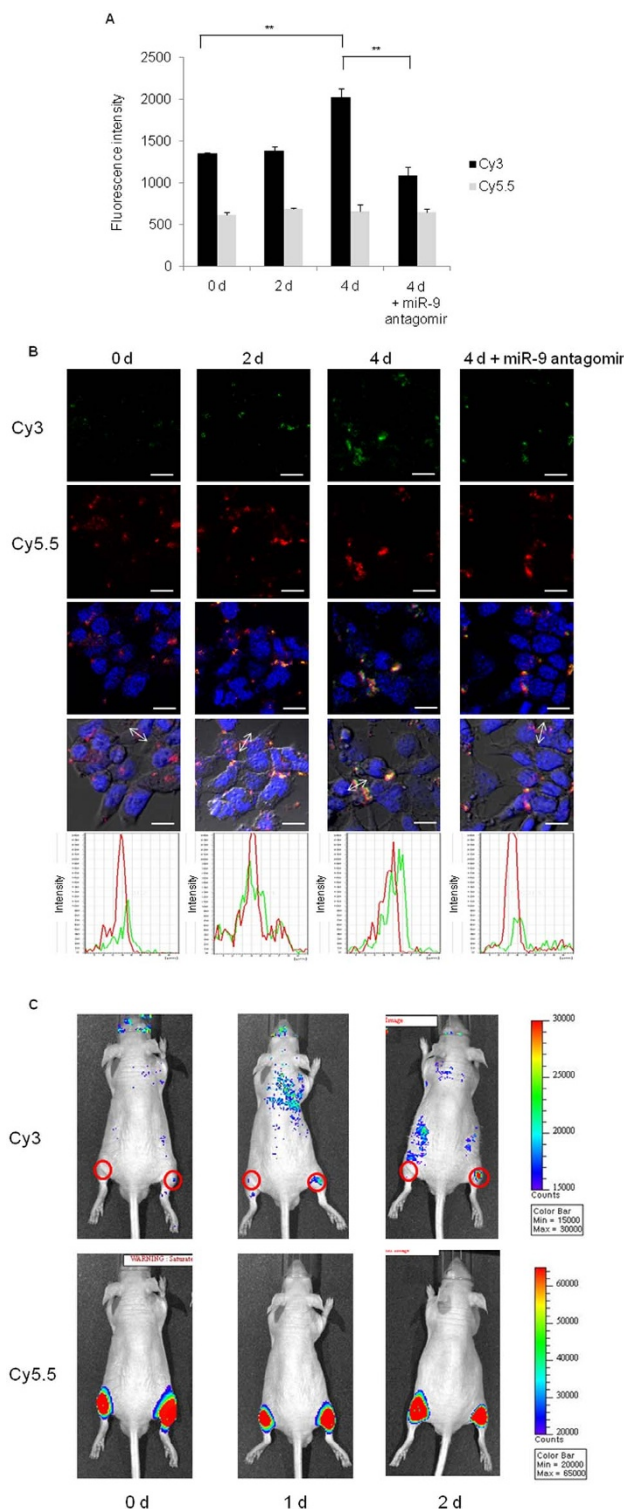


Figure 3 | *In vitro* and *in vivo* imaging of the ColoR9 MB during P19 cells neurogenesis. (A) Fluorescence intensity of the ColoR9 MB to sense endogenous miR-9 expression. P19 cells were induced into neuronal differentiation with RA. The ColoR9 MB was transfected into undifferentiated P19 cells (0 d) and 2-day- (2 d) and 4-day (4 d)-post-differentiated P19 cells. Additionally, 30 pmol of miR-9 antagonist (used as a control) was co-transfected with the ColoR9 MB into 4-day-post-differentiated P19 cells. Cy3 and Cy5.5 fluorescence intensities are displayed as means \pm standard deviations of triplicate samples (** $P < 0.005$). (B) Confocal microscopic analysis of the ColoR9 MB during P19 cell neuronal differentiation. The ColoR9 MB (30 pmol) was incubated on days 0, 2, and 4 after neuronal differentiation of P19 cells. Confocal microscopic images from the reporter probe (Cy3, green, Ex: 546 nm, Em: 563 nm) and the reference probe (Cy5.5, red, Ex: 683 nm, Em: 705 nm) were obtained for up to 4 days with or without additional incubation of miR-9 antagonist. Figures in the third and fourth rows were merged with DAPI and cellular morphology, respectively. Yellow was obtained by merging green from Cy3 and red from Cy5.5. Fluorescence intensity of Cy3 (green) and Cy5.5 (red) in the fifth row shows the line scan data along the line shown in the fourth row. Scale bar, 10 μ m. (C) *In vivo* image of the ColoR9 MB during P19 cell neurogenesis. A total of 1×10^7 P19 cells transfected with the ColoR9 MB were implanted into both thighs of nude mice (indicated by red circle). P19 cells only in the right thigh were induced to differentiate. *In vivo* fluorescence imaging of the reporter probe (Cy3, upper panel, Ex: 533 nm, Em: 580 nm) and the reference probe (Cy5.5, lower panel, Ex: 675 nm, Em: 720 nm) was acquired for 2 days.



attached even after hybridization with target molecules¹⁹. A linear-structured color-tunable MB can solve the problems by detaching the quencher molecule from the MB in the presence of target molecules²⁰.

In this study, we developed a linear-structured color-tunable miR-9 MB, ColoR9 MB, which was composed of a reporter probe with Cy3/BHQ1 and a reference probe with Cy5.5. Because the green fluorescence of the reporter probe showed miR-9 expression-dependent fluorescence recovery and the red fluorescence of the reference probe demonstrated invariable brightness regardless of miR-9 expression, the ColoR9 MB clearly visualized CHO and P19 cells with red in the absence of miR-9 and yellow in the presence of miR-9. *In vivo* imaging of the ColoR9 MB demonstrated a gradual increase in fluorescence recovery of the reporter probe during P19 cell neuronal differentiation due to a gradual increase in miR-9 expression which was bound to the miR-9 binding site and resulted in detachment of the quencher oligonucleotide from the ColoR9 MB. Red fluorescence activity remained strongly constant before and after P19 cell neurogenesis. As strong Cy5.5 fluorescence activity of the miR-9 insensitive dye was clearly visualized regardless of miR-9 expression, it provided an easy understanding of the low Cy3 signals of the miR-9 sensitive dye, which resulted from the absence of miR-9 before neurogenesis or in the weak presence of miR-9 during the early stage of neurogenesis. Such a color-tunable miR-9 imaging system could differentiate low fluorescence activity of the reporter probe resulting from low miR-9 expression and low transfection of the ColoR9 MB. The ColoR9 MB visualized relative quantitative miR-9 expression by providing the ratio of fluorescence activity of the reporter probe vs. the reference probe, which is frequently vague with an on/off-tunable MB sensor. Besides, such quantitative ratio during neurogenesis visualized the uneven localization of miR-9 expression in a single cell and unequal expression of miR-9 in P19 cells. These results demonstrate the high specificity of the ColoR9 MB that exhibited high sensitivity for sensing the miR-9 expression- and miR-9-regulating neurogenesis-dependent color changes.

Methods

Cell culture. CHO cells (Chinese hamster ovary cells) and P19 cells (mouse embryonic teratocarcinoma cell line) were purchased from the American Type Culture Collection (ATCC). CHO cells were cultured on growth media consisting of Dulbecco's modified Eagle's medium (DMEM) with 10% fetal bovine serum (FBS). P19 cells were maintained in DMEM containing 10% FBS, 1% antibiotics, non essential amino acid solution (NEAA, Sigma, St Louis, MO) and β -mercaptoethanol in a 5% CO₂-humidified chamber. For the induction of neuronal differentiation of P19 cells, the cells were cultured with DMEM/F12 (1:1) medium (Gibco, Grand Island, NY) containing N2 supplement (Gibco) and 0.5 mM all-trans-retinoic acid (RA, Sigma, St Louis, MO). After 2 days, the differentiation medium was replaced without RA.

Quantification of expression in miRNA. The expression of miR-9 was quantified by quantitative reverse polymerase chain reaction (qRT-PCR) using the total RNA obtained from CHO and P19 cells on the differentiation day. Total RNA was isolated from CHO and P19 cells using Trisol reagent (Invitrogen, Grand Island, NY). For qRT-PCR of mRNAs, 500 ng of RNA sample were reverse transcribed using the SuperscriptTM III first-strands synthesis system (Invitrogen, Grand Island, NY) for cDNA synthesis. The qRT-PCR was performed in triplicate using an iCycler (Bio-Rad, Hercules, CA) and SYBR Premix Ex TaqTM (2 \times ; Takara, Japan) at 95°C for 3 min and 40 cycles of 95°C for 15 s and 62°C for 30 s. The relative amounts of each mRNA were normalized versus β -actin primer.

For qRT-PCR of miRNAs, 200 ng of RNA were performed by using miR-Q-assay²¹. Each miRNA expression was represented relative to the expression of small RNA 5S rRNA, which was used as an internal control of the qRT-PCR. The expression data were presented as means of relative expression values obtained from three samples with standard deviation. For the comparison of the mean, a t-test was performed with a p-value of 0.005 as significance.

Confirmation of neuronal differentiation with immuno-fluorescence staining.

P19 cells were fixed with 4% formaldehyde for 20 min and washed three times for 10 min with PBS. The blocking and permeabilization procedures were simultaneously performed with a 10% normal goat serum reaction mixture and 0.1% Triton X-100 added to the cells for 60 min. The Oct4 or Tuj1 protein was detected by a 1:200 dilution of anti-Oct4 antibody (Chemicon, Millipore, Watford, UK) and a 1:1000 dilution of anti-Tuj1 antibody (Santa Cruz Biotechnology, Heidelberg, Germany) and incubated

overnight at 4°C. After three washing steps of 10 min each, Alexa Fluor secondary antibody conjugates were added and the mixture was incubated for 90 min. The cells were placed on a cover slip and mounted with aqueous mounting solution containing DAPI (Vector Laboratories, Inc., CA). The fluorescence signal was detected by confocal laser scanning microscopy (LSM 510; Carl Zeiss, Weimer, Germany).

Design of the ColoR9 MB. The sequences of miR-9, 5'-UCUUUGGUAUCUAG-CUGUAUGA-3', were obtained from the PicTar database (<http://pictar.mdc-berlin.de/>). The partially double-stranded ColoR9 MB with a miR-9 binding sequence which is reverse complementary against miR-9 was purchased from Bionics (Bionics, Inc, Koea) and synthesized as follows; a long oligonucleotide, 5'-Cy3-ccgcga TCATACAGCTAGATAACCAAAGAAAAAATCAACCTCC-Cy5.5-3' and a short oligonucleotide, 5'-TATGATcgcgg- BHQ1-3'. 30 pmol of the long oligonucleotide was annealed with 30 pmol of the short oligonucleotide to form the ColoR9 MB.

Transfection and fluorescence intensity. CHO cells were seeded onto a 24 well plate to the amount of 5×10^4 cells in each well. After 24 h, 30 pmol of the ColoR9 MB or 30 pmol of the long oligonucleotide was transfected to CHO cells with LipofectAMINE and Plus reagent (Invitrogen, Grand Island, NY). Mature miR-9 was applied to each well plate with various concentrations of 0, 1, 10, and 30 pmol. Mature miR-1 (30 pmol) was used as a negative control. After incubation for 3 h at 37°C, the cells were washed two times for 10 min at room temperature under mild shaking and lysed with RIPA buffer (Thermo Fisher Scientific Inc., Waltham, MA). The fluorescence was measured using Bio Tek Fluorescent Microplate Fluorometer (Synergy Mx, BioTeck Ltd, VT). In P19 cells, 30 pmol of the ColoR9 MB with or without 30 pmol of miR-9 antagonist was transfected to P19 cells 0, 2, and 4 days after the treatment of RA. The transfection procedure in P19 cells was the same as that in CHO cells. After incubation for 3 h at 37°C, the fluorescence intensity was measured with the previous method. All data are presented as the means \pm SD calculated from quadruple wells and significant differences between samples were assessed using a Student's t-test ($P < 0.005$).

Stability test of the ColoR9 MB. The ColoR9 MB (30 pmol) was added in PBS, Opti-MEM media and CHO cells and further incubated up to 2 days. To confirm the stability of the ColoR9 MB, miR-9 (30 pmol) was additionally treated into PBS, Opti-MEM media and CHO cells for 3 h at 37°C for 2 days after the incubation of the ColoR9 MB. The fluorescence intensity of the ColoR9 MB was measured using Bio Tek Fluorescent Microplate Fluorometer.

Confocal microscopy. CHO and P19 cells (5×10^4) were seeded into 4-well plates containing 25-mm-diameter cover glass and grown for 24 h at room temperature. The cells were transfected with 30 pmol of the long oligonucleotide or 30 pmol of the ColoR9 MB and then washed with phosphate-buffered saline (PBS) twice for 15 min. The cells were fixed with 500 ml of 3.7% formaldehyde (Sigma, St Louis, MO), washed three times with PBS for 10 min and cover-slipped with mounting medium containing a 40, 6-diamidino-2-phenylindole dihydrochloride (DAPI) solution (Vector Laboratories, Inc, CA). The cells were imaged by confocal laser scanning microscopy (Carl Zeiss LSM 510, Weimer, Germany) using filters specific for Cy3 (Excitation/Emission: 546/563 nm) and Cy5.5 (Excitation/Emission: 683/705 nm). The line intensity scan of the ColoR9 MB in CHO and P19 cells was achieved by scanning of 10 μ m distance. ROIs of confocal microscopy image from P19 cells during neurogenesis were selected using LSM Image Examiner and mean intensity of ROI values from two fluorescence signals were obtained. Mean intensity values were further normalized to compare the ROI fold ratio; intensity of Cy3 over intensity of Cy5.5.

***In vivo* fluorescence imaging.** All animals used in the *in vivo* experiments were housed under specific pathogen-free conditions and the experiments were approved by the institution's animal care and use committee of CHA University. For *in vivo* imaging of the ColoR9 MB, 200 pmol of the ColoR9 MB was transfected into 1×10^7 of P19 cells using LipofectAMINE and Plus reagent (Invitrogen, Grand Island, NY). After incubation for 3 h at 37°C, the cells were harvested and transplanted subcutaneously into the left and right thigh of a male BALB/c nude mouse (7 weeks old, $n = 3$). For neuronal differentiation, RA was administered in only right thigh. To acquire the image of the mouse, nude mouse were anesthetized with 2.5% of isofluorane, the optical imaging was performed at excitation: 533 and 675 nm and emission: 580 and 720 nm using the IVIS[®] spectrum imaging system (Caliper Life Sciences, MA). A camera was used to acquire captured images at constant exposures times (10 s). ROI values were normalized by intensity of RA treated right thigh over intensity of RA non-treated left thigh. The normalized value at day 0 was determined as a basal value, and used to analyze normalized values at day 2 and 4.

1. Noya, O., Patarroyo, M. E., Guzman, F. & Alarcon de Noya, B. Immunodiagnosis of parasitic diseases with synthetic peptides. *Curr. Protein Pept. Sci.* **4**, 299–308 (2003).
2. Fang, X., Li, J. J., Perlette, J., Tan, W. & Wang, K. Molecular beacons: novel fluorescent probes. *Anal. Chem.* **72**, 747A–753A (2000).
3. Wang, K. *et al.* Novel fluorescent molecular beacon DNA probes for biomolecular recognition. *In Biomedical Photonics Handbook: CRC Press* 57.51–57.52 (2003).



4. Solomon, B., Towards diagnosis and treatment of Alzheimer's disease. In Immunization Against Alzheimer's Disease and Other Neurodegenerative Disorders. Springer-Verlag 11–19 (2003).
5. Wienholds, E. & Plasterk, R. H. MicroRNA function in animal development. *FEBS Lett.* **579**, 5911–5922 (2005).
6. Bartel, D. P. MicroRNAs: target recognition and regulatory functions. *Cell* **136**, 215–233 (2009).
7. Kang, W. J. *et al.* Molecular beacon-based bioimaging of multiple microRNAs during myogenesis. *Biomaterials* **32**, 1915–1922 (2011).
8. Kim, J. K., Choi, K. J., Lee, M., Jo, M. H. & Kim, S. Molecular imaging of a cancer-targeting theragnostics probe using a nucleolin aptamer- and microRNA-221 molecular beacon-conjugated nanoparticle. *Biomaterials* **33**, 207–217 (2012).
9. Lee, J. Y. *et al.* Development of a dual-luciferase reporter system for in vivo visualization of MicroRNA biogenesis and posttranscriptional regulation. *J. Nucl. Med.* **49**, 285–294 (2008).
10. Ko, M. H. *et al.* Bioimaging of the unbalanced expression of microRNA9 and microRNA9* during the neuronal differentiation of P19 cells. *FEBS J.* **275**, 2605–2616 (2008).
11. Kim, H. J., Kim, Y. H., Lee, D. S., Chung, J. K. & Kim, S. In vivo imaging of functional targeting of miR-221 in papillary thyroid carcinoma. *J. Nucl. Med.* **49**, 1686–1693 (2008).
12. Ko, H. Y., Hwang do, W., Lee, D. S. & Kim, S. A reporter gene imaging system for monitoring microRNA biogenesis. *Nat. Protoc.* **4**, 1663–1669 (2009).
13. Varallyay, E., Burgyan, J. & Havelda, Z. MicroRNA detection by northern blotting using locked nucleic acid probes. *Nat. Protoc.* **3**, 190–196 (2008).
14. Krichevsky, A. M., King, K. S., Donahue, C. P., Khrapko, K. & Kosik, K. S. A microRNA array reveals extensive regulation of microRNAs during brain development. *RNA* **9**, 1274–1281 (2003).
15. Lagos-Quintana, M. *et al.* Identification of tissue-specific microRNAs from mouse. *Curr. Biol.* **12**, 735–739 (2002).
16. Zadran, S. *et al.* Fluorescence resonance energy transfer (FRET)-based biosensors: visualizing cellular dynamics and bioenergetics. *Appl. Microbiol. Biotechnol.* **96**, 895–902 (2012).
17. Packer, A. N., Xing, Y., Harper, S. Q., Jones, L. & Davidson, B. L. The bifunctional microRNA miR-9/miR-9* regulates REST and CoREST and is downregulated in Huntington's disease. *J. Neurosci.* **28**, 14341–14346 (2008).
18. Chen, A. K., Davydenko, O., Behlke, M. A. & Tsourkas, A. Ratiometric bimolecular beacons for the sensitive detection of RNA in single living cells. *Nucleic Acids Res.* **38**, e148 (2010).
19. Karlsen, K. K., Okholm, A., Kjems, J. & Wengel, J. A quencher-free molecular beacon design based on pyrene excimer fluorescence using pyrene-labeled UNA (unlocked nucleic acid). *Bioorg. Med. Chem.* **21**, 6186–6190 (2013).
20. Hwang do, W., Song, I. C., Lee, D. S. & Kim, S. Smart magnetic fluorescent nanoparticle imaging probes to monitor microRNAs. *Small* **6**, 81–88 (2010).
21. Sharbati-Tehrani, S., Kutz-Lohroff, B., Bergbauer, R., Scholven, J. & Einspanier, R. miR-Q: a novel quantitative RT-PCR approach for the expression profiling of small RNA molecules such as miRNAs in a complex sample. *BMC Mol. Biol.* **9**, 34 (2008).

Acknowledgments

This work was supported by the Bio & Medical Technology Development Program of the National Research Foundation (NRF) funded by the Korean government (MEST) (No. 2011-0019270 and No. 2013R1A2A2A01068140), the Next-Generation BioGreen 21 program (#PJ010002), Rural Development Administration and a grant of the Korea Healthcare technology R&D Project, Ministry of Health and Welfare (A120254).

Author contributions

S.K. and H.Y.K. planned the project, developed the color-tunable molecular beacon and wrote the manuscript. H.Y.K., J.Y.J. and J.J.K. contributed to acquire the *in vitro* image. J.L. Y.S.L. and H.H. conducted *in vivo* image. All authors discussed the results and commented on the manuscript.

Additional information

Supplementary information accompanies this paper at <http://www.nature.com/scientificreports>

Competing financial interests: The authors declare no competing financial interests.

How to cite this article: Ko, H.Y. *et al.* A color-tunable molecular beacon to sense miRNA-9 expression during neurogenesis. *Sci. Rep.* **4**, 4626; DOI:10.1038/srep04626 (2014).



This work is licensed under a Creative Commons Attribution-NonCommercial-NoDerivs 3.0 Unported License. The images in this article are included in the article's Creative Commons license, unless indicated otherwise in the image credit; if the image is not included under the Creative Commons license, users will need to obtain permission from the license holder in order to reproduce the image. To view a copy of this license, visit <http://creativecommons.org/licenses/by-nc-nd/3.0/>